Proapoptotic BAX and BAK regulate the type 1 inositol trisphosphate receptor and calcium leak from the endoplasmic reticulum

Scott A. Oakes*, Luca Scorrano†‡, Joseph T. Opferman*, Michael C. Bassik*, Mari Nishino*, Tullio Pozzan‡§, and Stanley J. Korsmeyer*¶

*Howard Hughes Medical Institute, Dana–Farber Cancer Institute, Brigham and Women's Hospital, Departments of Pathology and Medicine, Harvard Medical School, Boston, MA 02115; †Department of Biomedical Sciences, Dulbecco Telethon Institute, ‡Venetian Institute of Molecular Medicine, and §Department of Biomedical Sciences, University of Padua, 35121 Padua, Italy

Contributed by Stanley J. Korsmeyer, November 9, 2004

Proapoptotic BCL-2 family members BAX and BAK are required for the initiation of mitochondrial dysfunction during apoptosis and for maintaining the endoplasmic reticulum (ER) Ca^{2+} stores necessary for Ca^{2+}-dependent cell death. Conversely, antiapoptotic BCL-2 has been shown to decrease Ca^{2+} concentration in the ER. We found that *Bax*$^{-/-}$*Bak*$^{-/-}$ double-knockout (DKO) cells have reduced resting ER Ca^{2+} levels because of increased Ca^{2+} leak and an increase in the Ca^{2+}-permeable, hyperphosphorylated state of the inositol trisphosphate receptor type 1 (IP3R-1). The ER Ca^{2+} defect of DKO cells is rescued by RNA interference reduction of IP3R-1, supporting the argument that this channel regulates the increased Ca^{2+} leak in these cells. BCL-2 and IP3R-1 physically interact at the ER, and their binding is increased in the absence of BAX and BAK. Moreover, knocking down BCL-2 decreases IP3R-1 phosphorylation and ER Ca^{2+} leak rate in the DKO cells. These findings support a model in which BCL-2 family members regulate IP3R-1 phosphorylation to control the rate of ER Ca^{2+} leak from intracellular stores.

Apoptosis is often regulated by signals arising from or converging on intracellular organelles, such as mitochondria or the endoplasmic reticulum (ER) (1). In mammalian cells, the BCL-2 family of proteins plays a central role in modulating mitochondrial-dependent apoptosis. Both pro- and antiapoptotic BCL-2 family members are critical death regulators proximal to mitochondria and irreversible cell damage (2).

There is growing evidence that the BCL-2 family controls apoptosis from the ER, the main Ca^{2+} cellular store. Recently, it has become apparent that apoptosis can be positively or negatively influenced by subtle changes in Ca^{2+} concentration within intracellular compartments. Cellular Ca^{2+} overload or perturbations of intracellular Ca^{2+} stores may lead to cytotoxic stress and trigger cell death (3). Mitochondria and ER are physically and physiologically coupled, perhaps best illustrated by the crosstalk between these organelles during Ca^{2+} signaling (4, 5). After inositol trisphosphate (IP3)-mediated release of Ca^{2+} from the ER through the IP3 receptor, high-Ca^{2+} microdomains (estimated to be in the range of 50–100 μM) are generated at the tight ER–mitochondrial junctions, activating the low-affinity mitochondrial Ca^{2+} uniporter and resulting in mitochondrial Ca^{2+} uptake (5). Mitochondrial Ca^{2+} uptake regulates the shape and amplitude of cytosolic Ca^{2+} transients and also modulates Ca^{2+}-dependent mitochondrial Krebs cycle enzymes (6) as well as permeability transition, ascribed to an inner mitochondrial membrane channel that appears to play a role in cell death in response to selected stimuli (7).

Evidence is accumulating to support a central role for the BCL-2 family in regulating ER Ca^{2+} concentration ($[Ca^{2+}]_{er}$). BCL-2 overexpression has been shown to reduce ER Ca^{2+} stores and diminish capacitative Ca^{2+} entry (CCE) after ER Ca^{2+} release (8, 9). Proapoptotic BAX and BAK localize to both mitochondria and ER, and overexpression of these proteins has been shown to promote Ca^{2+} mobilization from the ER to the mitochondrion during apoptosis (10). Moreover, cells deficient in BAX and BAK have a dramatically reduced $[Ca^{2+}]_{er}$ and secondarily decreased Ca^{2+} uptake by mitochondria, and are highly resistant to Ca^{2+}-dependent death stimuli. Genetic correction of the ER Ca^{2+} defect in double-knockout (DKO) cells by overexpressing sarcoplasmic–ER Ca^{2+} adenosine triphosphatase (SERCA) restored apoptosis in response to Ca^{2+}-mobilizing stimuli, including oxidative stress (11).

Uncertainties remain regarding the mechanism by which BCL-2 family members modulate Ca^{2+} concentration in intracellular stores. It has been reported that BCL-2 overexpression reduces CCE, which replenishes Ca^{2+} stores after their discharge (12). This reduction is due not to an intrinsic modulation of the Ca^{2+} conductivity of the CCE channels but to a net decrease in the number of functionally active channels on the cell surface (13). Conversely, different mechanisms have been proposed for the action of BCL-2 family proteins at the level of the ER. In certain cell lines, BCL-2 overexpression has resulted in lower levels of calreticulin and of SERCA2b (13). Overexpression of the antiapoptotic family member BCL-XL has been reported to decrease the IP3-releasable Ca^{2+} pool and reduce expression of IP3 receptor type 1 (IP3R-1) in lymphocytes (14). Increased levels of BCL-2 have been reported to enhance Ca^{2+} leak from the ER (8, 9). One proposal is that this leak might be a consequence of an intrinsic Ca^{2+} conductance by BCL-2 (8). However, in the absence of proapoptotic BCL-2 family members BAX and BAK, levels of ER proteins involved in Ca^{2+} uptake, buffering, and release and the CCE are unchanged (11). Moreover, studies of the electrophysiological properties of BAX concluded that it lacked any specific conductivity for divalent cations (15). These data suggested that a different mechanism is responsible for the reduction of $[Ca^{2+}]_{er}$ in DKO cells.

Here we investigated the mechanism of $[Ca^{2+}]_{er}$ reduction in DKO cells. Passive leak of ER Ca^{2+} after SERCA inhibition is increased in the absence of BAX and BAK and correlates with hyperphosphorylation of IP3R-1, a modification known to augment the ion-conducting activity of this Ca^{2+} channel (16, 17). We found that BCL-2 and IP3R-1 physically interact at the ER membrane, and their binding is enhanced in DKO cells that lack BAX and BAK. Moreover, RNA interference (RNAi)-targeted reduction of BCL-2 led to decreased IP3R-1 phosphorylation and, similar to directly knocking down expression of IP3R-1,

CELL BIOLOGY

Abbreviations: ER, endoplasmic reticulum; IP3, inositol trisphosphate; $[Ca^{2+}]_{er}$, ER Ca^{2+} concentration; CCE, capacitative Ca^{2+} entry; IP3R-1, inositol trisphosphate receptor type 1; DKO, double-knockout; SERCA, sarcoplasmic–ER Ca^{2+} adenosine triphosphatase; RNAi, RNA interference; erAEQ, ER-targeted aequorin; tBuBHQ, 2,5-di(*tert*-butyl)-1,4-benzohydroquinone; MEFs, mouse embryo fibroblasts.

¶To whom correspondence should be addressed. E-mail: stanley_korsmeyer@dfci.harvard.edu.

© 2004 by The National Academy of Sciences of the USA

corrected ER Ca^{2+} leak and restored Ca^{2+} levels in DKO cells. Together, these findings support the argument that the ratio of pro- versus antiapoptotic BCL-2 family members can control $[Ca^{2+}]_{er}$ through IP3R-1–mediated Ca^{2+} leak.

Materials and Methods

Cytosolic Ca^{2+} Measurements. Cells (10^6) were incubated at 37°C in Hanks' balanced salt solution (HBSS, Sigma) containing 10% FCS and Fura-2 AM (1 μM, Molecular Probes). After 30 min, cells were trypsinized and resuspended in HBSS at a density of 10^6 per ml. Ratiometric Ca^{2+} measurements were performed at λ_{em} 340 ± 5 and 380 ± 5, and λ_{ex} 510 ± 15 nm at 37°C in an LS50B fluorimeter (PerkinElmer) equipped with fast filter and magnetic stirring. Fura-2 ratio values were converted into Ca^{2+} concentrations (18), by using K_d = 225 nM for Ca^{2+}.

ER-Targeted Aequorin (erAEQ) Transfection and Measurements. Cells (10^5) were grown on 13-mm round glass coverslips and, after 24 h, were transfected with erAEQ. To obtain reliable $[Ca^{2+}]_{er}$ measurements, ER stores were depleted before and during reconstitution of erAEQ. Reconstitution, measurement, and calibration were performed as described (8, 11).

Subcellular Fractionation and Immunoprecipitation. Cells (10^9) were harvested, resuspended in an isotonic buffer [10 mM Tris, pH 7.6/100 mM $CaCl_2$/200 mM sucrose], and disrupted by Dounce homogenization followed by 20 strokes through a 30 gauge needle. The homogenate was spun at 800 × *g* for 10 min, and the supernatant was recovered and further centrifuged for 10 min at 8,000 × *g*. The resulting pellet (mitochondrial fraction) was collected and the supernatant was further spun for 1 h and 30 min at 28,000 × *g*. The resulting pellet constituted the microsomal ER fraction and the supernatant constituted the cytosolic fraction. Before immunoprecipitation, ER fractions were solubilized in 1% 3-[(3-cholamidopropyl)dimethylammonio]-1-propanesulfonate (CHAPS)-containing buffer [5 mM sodium phosphate, pH 7.4/2.5 mM EDTA/100 mM NaCl/1 mM NaF/1 mM sodium orthovanadate] and 1 mg of precleared protein was incubated with anti-BCL-2 antibody (3F11) bound to protein A/G agarose beads (Santa Cruz Biotechnology). Protein complexes were separated by SDS/PAGE, transferred onto poly(vinylidene difluoride) membranes, and probed for the indicated proteins.

Western Blotting. To prepare total cellular lysates, cells (10^6) were disrupted in RIPA buffer [150 mM NaCl/1% Nonidet P-40/0.5% deoxycholate/0.1% SDS/50 mM Tris, pH 8.0/1 mM NaF/1 mM sodium orthovanadate] in the presence of complete protease-inhibitor mixture (Sigma). Extracted proteins (45 μg) were separated by SDS/4–12% or 3–8% PAGE (NuPAGE, NOVEX, San Diego), transferred onto poly(vinylidene difluoride) membranes (Millipore), and probed by using the following antibodies: anti-Mn-superoxide dismutase (1:1,000, Stressgen Biotechnologies, Victoria, BC, Canada), anti-IP3R-1 (1:1,000, Affinity BioReagents, Golden, CO), anti-IP3R-3 (1:500, BD Pharmingen), anti-phosphoserine (1:500, Zymed), anti-IP3R-1 phosphoserine-1755 (19), and anti-BCL-2 (1:250, 3F11). Isotype-matched, horseradish-peroxidase-conjugated secondary antibodies were used, followed by detection with chemiluminescence (PerkinElmer).

RNAi. RNAi (20 μM) sequence corresponding to a 21-nt region from murine Bcl-2 (GenBank accession no. M16506; nucleotides 64–86), IP3R-1 (GenBank accession no. NM-010585; nucleotides 505–523, 2254–2272, 3680–3698, and 5122–5140), and IP3R-3 (GenBank accession no. NM_080553; nucleotides 1114–1132, 1125–1143, 1219–1237, and 1459–1477) (Dharmacon Research, Lafayette, CO) were annealed by incubation in 100 mM KCH_3CO_2/30 mM Hepes–KOH (pH 7.4)/2 mM $Mg(CH_3CO_2)_2$ for 1 min at 90°C, followed by incubation for 1 h at 37°C. Double-strand siRNA corresponding to a region of green fluorescence protein (5′-GCAGCACGACUUCUUCAAGU-3′) was used as a control. Fifty percent confluent cells were transfected by using Oligofectamine (Invitrogen) at 0.2 nM siRNA duplex per well (six-well plate) in serum-free medium for 4 h and then cultured overnight in the presence of serum (10%). All measurements were performed 24–48 h after RNAi addition.

Results

ER Ca^{2+} Leak Is Increased in the Absence of BAX and BAK. We previously reported that the proapoptotic proteins BAX and BAK partially localize to ER membranes and that $Bax^{-/-}Bak^{-/-}$ (DKO) cells have a reduced resting free Ca^{2+} concentration in the ER ($[Ca^{2+}]_{er}$), which results in decreased uptake of Ca^{2+} by mitochondria after ER Ca^{2+} release (11). Steady-state free $[Ca^{2+}]_{er}$ reflects an equilibrium between active Ca^{2+} accumulation by SERCA pumps and passive leak across the ER membrane. Levels of expression of proteins involved in Ca^{2+} buffering, uptake, and release and the rate of Ca^{2+} uptake by SERCA were unchanged in DKO cells (11). Therefore, we examined regulation of ER Ca^{2+} leak in DKO cells.

To measure Ca^{2+} leak from the ER, we targeted the aequorin Ca^{2+} photoreporter (erAEQ) to the ER lumen and monitored leak after inhibition of SERCA uptake by the reversible inhibitor 2,5-di(*tert*-butyl)-1,4-benzohydroquinone (tBuBHQ) (8). After $[Ca^{2+}]_{er}$ depletion, Ca^{2+} was returned to the perfusate of WT and DKO cells. Once steady-state $[Ca^{2+}]_{er}$ was reached, tBuBHQ was added, and the decline in $[Ca^{2+}]_{er}$ was monitored (Fig. 1*A*). To directly compare the leak at equivalent $[Ca^{2+}]_{er}$ in DKO versus WT cells, we plotted the leak rate $d[Ca^{2+}]/dt$ as a function of $[Ca^{2+}]_{er}$. The rate of decrease in ER Ca^{2+} at each individual $[Ca^{2+}]_{er}$ proved significantly greater in DKO than in WT cells (Fig. 1*B*). This observation indicates that a constitutively higher ER Ca^{2+} leak exists in DKO cells, which would result in a lower steady-state $[Ca^{2+}]_{er}$ and impaired release in response to IP3, as previously observed (11).

DKO Cells Display Increased Phosphorylation of IP3R-1 at the ER. The mechanism of ER Ca^{2+} leak is incompletely understood and may differ among various cell types (20). However, some investigators have reported that the IP3R-1 represents at least one pathway involved in ER Ca^{2+} leak (16). Ca^{2+} release through the IP3R can be influenced by many factors, including phosphorylation and local Ca^{2+} concentration (21). IP3R-1 channel conductivity is regulated through phosphorylation at numerous sites by protein kinase A (PKA), protein kinase C (PKC), and calcium/calmodulin-dependent protein kinase II, among others (22). For example, phosphorylation of serine-1755 on IP3R-1 by PKA has been found to increase the open probability and, hence, the Ca^{2+} permeability of this channel (23). Consequently, we separated cells into mitochondria, ER, and cytosol-enriched fractions and examined the phosphorylation status of the IP3R-1. Whereas the total amount of IP3R-1 was comparable, DKO cells consistently displayed an ≈5-fold increase in the phosphorylation of this Ca^{2+} channel as detected with an anti-phosphoserine antibody (Fig. 1*C*). Moreover, by using an antibody specific against phosphorylated serine-1755 of IP3R-1 (19), the predominant and highly conserved PKA phosphorylation site on the receptor, we noted a 4-fold increase in the DKO compared with WT cells (Fig. 1*C*). Therefore, serine-1755 represents at least one site on the IP3R-1 that is hyperphosphorylated in the absence of BAX and BAK. The increased phosphorylation status of IP3R-1 in the DKO cells suggested the possibility that this Ca^{2+} channel may be dysregulated and may contribute to ER Ca^{2+} leak in the absence of BAX and BAK.

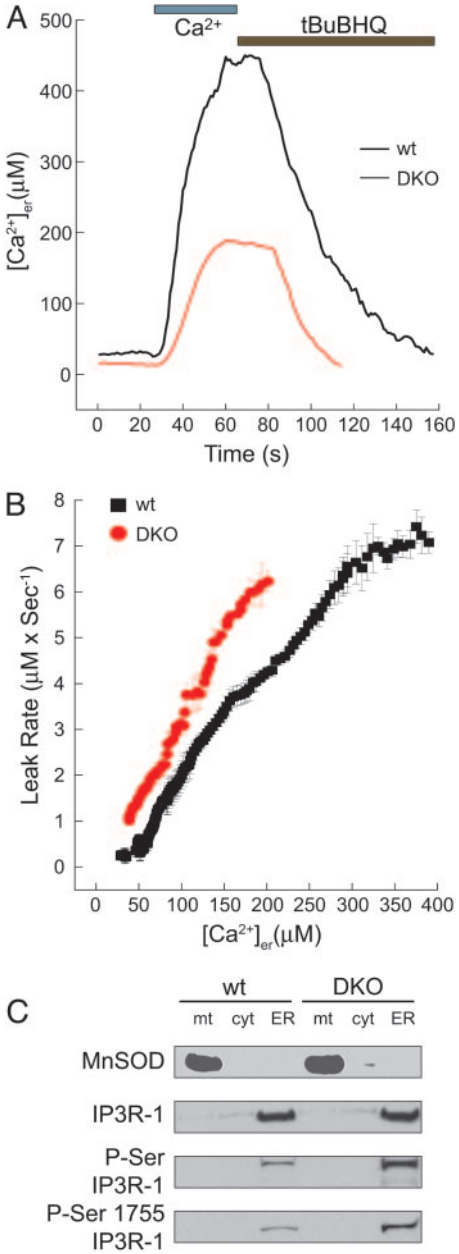

Fig. 1. Enhanced $[Ca^{2+}]_{er}$ leak in DKO MEFs is associated with increased phosphorylation of IP3R-1. (*A*) Representative recordings of erAEQ monitored $[Ca^{2+}]_{er}$ changes of ER Ca^{2+}-depleted WT and DKO in response to perfusion with 1 mM $CaCl_2$ buffer and with the SERCA inhibitor tBuBHQ (100 μM). (*B*) $[Ca^{2+}]_{er}$ changes were monitored with erAEQ in WT and DKO MEFs, and Ca^{2+} leak was measured as first-order derivative ±SE of $[Ca^{2+}]_{er} = f(t)$ after addition of the SERCA inhibitor tBuBHQ (100 μM); data were calculated from five experiments and plotted against the corresponding individual $[Ca^{2+}]_{er}$ ± SE. (*C*) Subcellular fractions from WT and DKO MEFs were separated by SDS/3–8% or 4–12% PAGE, and immunoblots for the mitochondrial marker Mn-superoxide dismutase (MnSOD), IP3R-1, phosphorylated serine (P-Ser) IP3R-1, and phosphorylated serine-1755 IP3R-1 were performed. mt, mitochondria; cyt, cytosol.

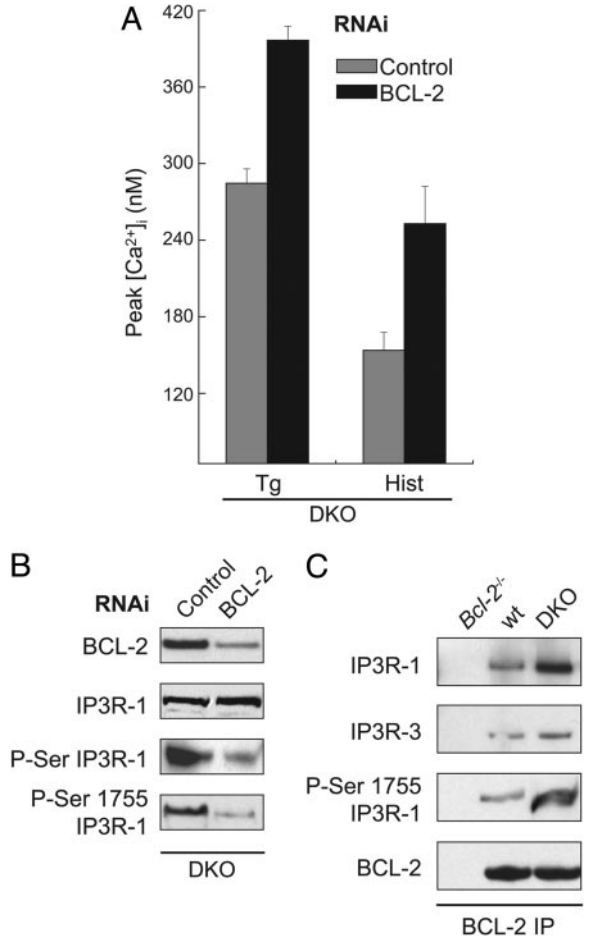

Fig. 2. Knocking down BCL-2 expression reduces phosphorylation of IP3 receptor type 1 and increases Ca^{2+} release in DKO cells. (*A*) Peak intracellular Ca^{2+} concentration ($[Ca^{2+}]_i$) as measured by Fura-2 in response to thapsigargin (Tg) (200 nM) or histamine (Hist) (100 μM) in DKO mouse embryo fibroblasts (MEFs) transfected with control (gray bars) or *Bcl-2* (black bars) RNAi 24 h before measurement. (*B*) Immunoblot of BCL-2 in total cellular lysates, or IP3R-1, phosphorylated serine (P-Ser) IP3R-1, and phosphorylated serine-1755 IP3R-1 in ER fractions of DKO MEFs 24 h after transfection with control or *Bcl-2* RNAi. (*C*) BCL-2 immunoprecipitation from ER fractions of *Bcl-2*$^{-/-}$, WT, and DKO MEFs. Immunoprecipitated complexes were then transferred to a membrane and blotted with antibodies against IP3R-1, IP3R-3, phosphorylated serine-1755 IP3R-1, and BCL-2.

BCL-2 Loss-of-Function Reverses the Effects of BAX and BAK Deficiency on IP3R-1 Phosphorylation and ER Ca^{2+} Release. Uncertainty exists as to whether antiapoptotic BCL-2 family members possess inherent activities beyond opposing (through binding and sequestering) proapoptotic members (24). Of note, BCL-2 has been implicated in regulating ER Ca^{2+} homeostasis, although the exact mechanism remains uncertain (25). For example, BCL-2 was recently reported to bind to the IP3 receptor and regulate IP3-mediated Ca^{2+} release from the ER (26). Others (8, 9) have found that overexpression of BCL-2 resulted in lower steady-state $[Ca^{2+}]_{er}$ and, therefore, diminished releasable Ca^{2+}. Consequently, we asked whether unopposed BCL-2 activity in DKO cells could account for the reduced $[Ca^{2+}]_{er}$ in the absence of BAX and BAK. We took a loss-of-function approach using RNAi, which reduced BCL-2 protein levels in DKO cells by ≈80% (Fig. 2*B*). The peak $[Ca^{2+}]_i$ in response to thapsigargin or histamine was significantly increased when BCL-2 was decreased (Fig. 2*A*), suggesting substantial correction of ER Ca^{2+} stores. Moreover, the increased phosphorylation of IP3R-1 observed in DKO cells by using either an anti-phosphoserine antibody or an antibody specific against phosphorylated serine-1755 was substantially reduced by "knocking down" BCL-2 (Fig. 2*B*).

Because changes in BCL-2 expression altered peak $[Ca^{2+}]_i$ and the phosphorylation status of IP3R-1, we explored whether the

CELL BIOLOGY

two proteins could physically interact in MEFs at the ER and, if so, whether this interaction was regulated by the presence of BAX and BAK. ER membranes isolated from *Bcl-2*$^{-/-}$ (negative control), WT, and DKO MEFs were solubilized in 3-[(3-cholamidopropyl)dimethylammonio]-1-propanesulfonate (CHAPS)-based buffer and immunoprecipitated with anti-murine BCL-2 antibody. The immunoprecipitated complexes were separated by SDS/PAGE and developed for IP3R-1 and IP3R-3. Both IP3R-1 and IP3R-3 were pulled down with BCL-2, suggesting that BCL-2 and the IP3 receptors are in a macromolecular complex at the ER membrane (Fig. 2*C*). Probing the immunoprecipitated complexes with an antibody against phosphorylated serine-1755 of the IP3R-1, we found that at least some of the IP3R-1 in association with BCL-2 was phosphorylated at this site (Fig. 2*C*). Moreover, the binding of IP3R-1 to BCL-2 was clearly increased in the absence of BAX and BAK (Fig. 2*C*). This enhanced association between BCL-2 and IP3R-1 in DKO cells correlates with the observation that unopposed BCL-2 modulates the phosphorylation and, hence, the Ca^{2+}-conducting status of IP3R-1. In total these results support the argument that the ratio of pro- to antiapoptotic BCL-2 members reciprocally regulates the phosphorylation status of IP3R-1 and the level of ER Ca^{2+}.

Knocking Down IP3R-1 Restores Thapsigargin-Mediated ER Ca^{2+} Release in DKO Cells. To assess whether the hyperphosphorylated IP3R-1 observed in DKO cells was contributing to the increased ER Ca^{2+} leak measured in these cells (Fig. 1*B*), we designed RNAi sequences against IP3R-1 or IP3R-3 that selectively knocked down protein expression of either receptor isoform (singly or in combination with BCL-2 RNAi) by >90% (Fig. 3*A*). To check whether this degree of reduction interferes with the physiological response of the cell to IP3, peak $[Ca^{2+}]_i$ was measured in response to the IP3-generating agonist histamine in WT cells transfected with RNAi targeted against IP3R-1, IP3R-3, or both IP3R-1/IP3R-3. Knocking down either isoform of the IP3 receptor led to a significant reduction in the cytosolic Ca^{2+} increase as measured by Fura-2 in response to histamine, and this reduction was even more pronounced when both isoforms were targeted with RNAi (Fig. 3*B*). Thus, the level of reduction in IP3R expression achieved by targeted RNAi significantly affects IP3-mediated Ca^{2+} release from the ER.

We next tested whether reducing IP3R-1 or IP3R-3 levels restored thapsigargin-releasable Ca^{2+} stores in DKO cells. RNAi targeted against IP3R-1 or BCL-2 increased thapsigargin-mediated Ca^{2+} release to a similar extent in DKO cells, whereas knocking down IP3R-3 had no effect (Fig. 3*C*). BCL-2 RNAi, which decreases the phosphorylation status of the IP3R-1 (Fig. 2*B*), did not further increase Ca^{2+} release when added to IP3R-1 RNAi (Fig. 3*C*), suggesting that the activities of BCL-2 and IP3R-1 are responsible for reduced ER Ca^{2+} release in DKO cells.

BCL-2 and IP3R-1 Regulate ER Ca^{2+} Leak and Steady-State $[Ca^{2+}]_{er}$ in DKO Cells. We then asked whether IP3R-1 or BCL-2 could account for the increased ER Ca^{2+} leak and reduced steady-state $[Ca^{2+}]_{er}$ in DKO cells. erAEQ showed that RNAi targeted against IP3R-1 but not IP3R-3 restored steady-state $[Ca^{2+}]_{er}$ in DKO MEFs to near WT levels (Fig. 4*A* and data not shown); however, knocking down IP3R-1 in WT cells had little effect on $[Ca^{2+}]_{er}$ levels. Likewise, BCL-2-targeted RNAi significantly increased $[Ca^{2+}]_{er}$ in DKO cells. Interestingly, knocking down both BCL-2 and IP3R-1 together in DKO cells did not produce any additive increase in $[Ca^{2+}]_{er}$, consistent with these proteins working in a linear pathway to control ER Ca^{2+}. After reaching $[Ca^{2+}]_{er}$ steady state, leak was measured after addition of tBuBHQ to the perfusate. Knocking down IP3R-1 significantly reduced ER Ca^{2+} leak in DKO cells to an intermediate level between that of WT and DKO cells transfected with control RNAi (Fig. 4*B*), but IP3R-1 RNAi had no significant effect on ER Ca^{2+} leak in WT cells (data not shown). Likewise, reduction of BCL-2 in DKO cells also decreased ER Ca^{2+} leak (Fig. 4*B*).

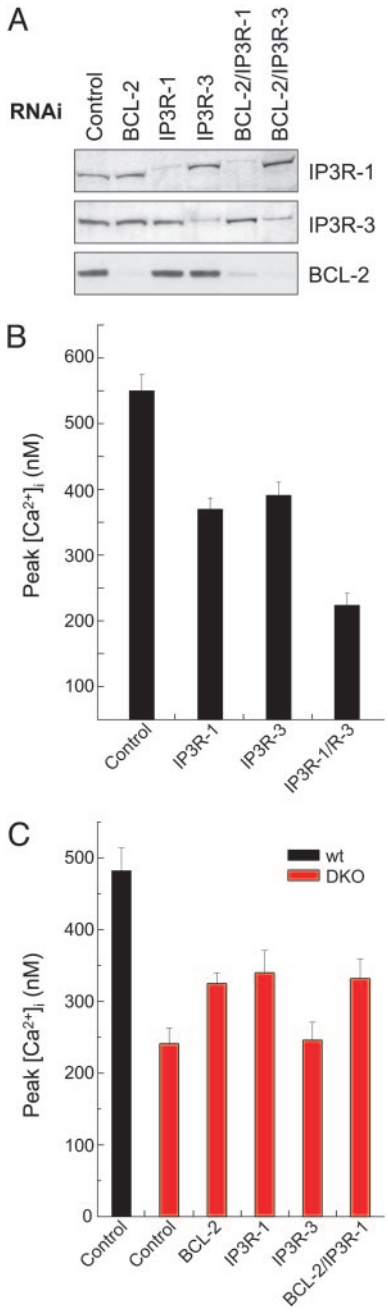

Fig. 3. Selective knockdown of hyperphosphorylated IP3R-1 substantially restores thapsigargin-mediated Ca^{2+} release in DKO cells. (*A*) Whole cell lysates were prepared from WT MEFs after a 24-h transfection with control, BCL-2, IP3R-1, or IP3R-3 RNAi or combinations thereof. Lysates were then immunoblotted for IP3R-1 (*Top*), IP3R-3 (*Middle*), and BCL-2 (*Bottom*) expression. (*B*) Peak $[Ca^{2+}]_i$ as measured by Fura-2 in response to histamine (100 μM) in the absence of extracellular Ca^{2+} in WT MEFs 24 h posttransfection with indicated RNAi sequence(s). (*C*) Peak $[Ca^{2+}]_i$ as measured by Fura-2 in response to thapsigargin (200 nM) in the absence of extracellular Ca^{2+} for WT and DKO MEFs 24 h posttransfection with indicated RNAi sequence(s). Peak $[Ca^{2+}]_i$ values for BCL-2, IP3R-1, and combined IP3R-1/BCL-2 RNAi-transfected DKO cells are significantly increased compared with control-transfected DKO cells ($P < 0.05$; Student's *t* test).

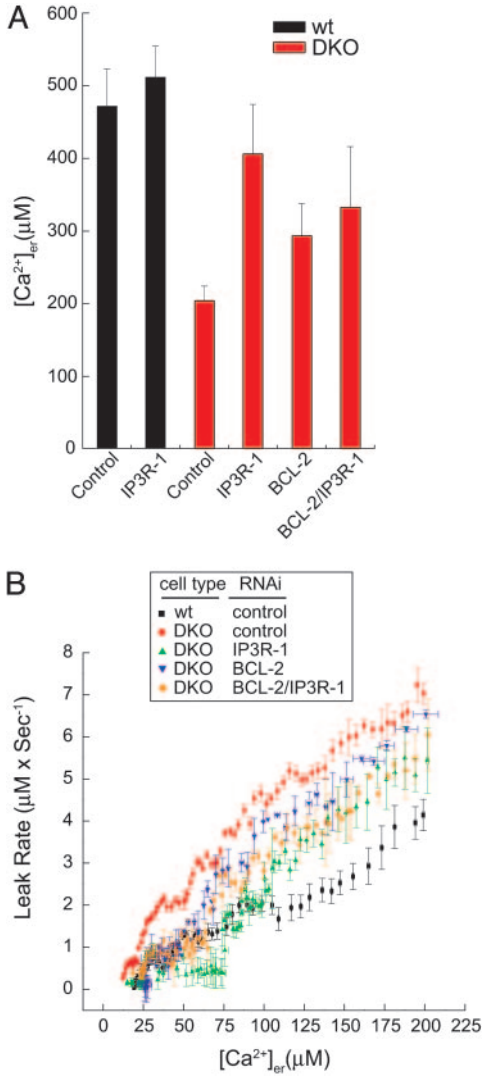

Fig. 4. Knockdown of BCL-2 or IP3R-1 in DKO cells leads to reduced ER Ca^{2+} leak and increased $[Ca^{2+}]_{er}$. (*A*) Steady-state $[Ca^{2+}]_{er}$ as measured by erAEQ in WT and DKO MEFs 48 h posttransfection with indicated RNAi sequence(s). $[Ca^{2+}]_{er}$ values for BCL-2, IP3R-1 and combined IP3R-1/BCL-2 RNAi-transfected DKO cells are significantly increased compared with control-transfected DKO cells ($P < 0.05$; Student's *t* test). The difference in $[Ca^{2+}]_{er}$ between BCL-2- and IP3R-1 RNAi-transfected DKO cells is not statistically significant. (*B*) $[Ca^{2+}]_{er}$ changes were monitored with erAEQ in WT and DKO transfected with the indicated RNAi sequences, and Ca^{2+} leak was measured as first-order derivative ± SE of $[Ca^{2+}]_{er} = f(t)$ after addition of tBuBHQ (100 μM); data were calculated from six experiments and plotted against the corresponding individual $[Ca^{2+}]_{er}$ ± SE.

These data suggest that, in the absence of BAX and BAK, BCL-2 and IP3R-1 contribute to ER Ca^{2+} leak. Knocking down both IP3R-1 and BCL-2 in combination did not provide any additive effect on the Ca^{2+} leak rate, consistent with the inability of this combination to further increase steady-state $[Ca^{2+}]_{er}$.

Discussion

Apoptosis is controlled by the multidomain proapoptotic proteins BAX and BAK either at the mitochondria, where these proteins are activated by BH3-only molecules to induce cytochrome *c* release, or at the ER, where they regulate $[Ca^{2+}]_{er}$ and Ca^{2+}-dependent death signals (3, 11). How these molecules perform such diverse functions is a critical remaining question. Here we explored the mechanism by which ablation of BAX and BAK results in lowered $[Ca^{2+}]_{er}$. The expression level of proteins known to be involved in Ca^{2+} buffering, uptake, and release was unchanged in $Bax^{-/-}Bak^{-/-}$ DKO cells (11). We used a combination of genetics, physiology, and biochemistry to clarify the mechanisms that lower steady-state $[Ca^{2+}]_{er}$ in DKO cells. $Bax^{-/-}Bak^{-/-}$ cells displayed an increase in the calcium-conducting, hyperphosphorylated state of the IP3R-1, as detected with a nonspecific phosphoserine antibody and an antibody specific to the major PKA phosphorylation site (serine-1755) on the receptor. We found that, in the absence of BAX and BAK, hyperphosphorylation of IP3R-1 is associated with an increased passive leak of Ca^{2+}, resulting in lower steady-state $[Ca^{2+}]_{er}$. Notably, RNAi targeted against IP3R-1 corrected the increased leak and restored ER Ca^{2+} levels in DKO but did not affect $[Ca^{2+}]_{er}$ or Ca^{2+} leak in WT cells. This result provides genetic evidence for a role of IP3R-1 in modulating Ca^{2+} leak from the ER in this specific setting that interfaces with the apoptotic pathway.

The molecular mechanisms that account for the passive leak of Ca^{2+} from the ER are under active investigation (20). Candidates include the translocon pore complex in the ER membrane (27, 28) and the IP3R-1 (16). In isolated cerebellar microsomes, PKC-mediated phosphorylation of IP3R-1 increases Ca^{2+} leak, whereas dephosphorylation of IP3R-1 by calcineurin decreases Ca^{2+} leak (16). However, in chicken DT-40 cells, ablation of all IP3R isoforms did not affect cytosolic peak Ca^{2+} in response to thapsigargin, although steady-state $[Ca^{2+}]_{er}$ and leak were not directly measured in this study (29). It has also been reported (30, 31) that pharmacologic inhibition of IP3R with either heparin or xestospongin did not affect basal calcium leak. It could be argued that the selectivity of pharmacologic inhibitors for the IP3R is uncertain. Furthermore, whereas these inhibitors are thought to block active Ca^{2+} release from the ER in response to IP3, it is less certain whether they block passive leak through the IP3R channel. Our data suggest that, at least in cells with reset apoptotic susceptibility, IP3R-1 plays a role in determining Ca^{2+} leak from the ER.

Similar to ablation of BAX and BAK, overexpression of antiapoptotic BCL-2 has been reported (8, 9) to increase passive Ca^{2+} leak from the ER, resulting in diminished intracellular Ca^{2+} stores and to protect cells from Ca^{2+}-dependent apoptotic stimuli (8). Roles for antiapoptotic BCL-2 members that result from binding and sequestering proapoptotic members or that represent independent functions remain under investigation (24). The inactive, phosphorylated form of BCL-2 predominantly localizes to the ER, and phosphorylation of BCL-2 inhibits its ability to lower $[Ca^{2+}]_{er}$, bind BH3-only members, and inhibit Ca^{2+}-dependent apoptosis (32). Consequently, we asked whether BCL-2 could influence $[Ca^{2+}]_{er}$ in the absence of BAX and BAK. Knocking down BCL-2 expression in DKO cells significantly reduced phosphorylation of IP3R-1, decreased ER Ca^{2+} leak, and increased steady-state $[Ca^{2+}]_{er}$. Thus, BCL-2 can also influence $[Ca^{2+}]_{er}$ independent of, and perhaps downstream of, BAX and BAK.

Members of the BCL-2 family are found in regulatory complexes at the outer mitochondrial membrane. BAK is retained in its inactive conformation by a specific interaction with the voltage-dependent anion channel-2 (33). BAD nucleates a holoenzyme complex with PKA, PP1α, WAVE-1, and glucokinase at the mitochondrion (34). We found that BCL-2 can physically interact with IP3R-1 at the ER membrane and that this interaction is enhanced when BAX and BAK are not present. Therefore, BAX and BAK may normally regulate $[Ca^{2+}]_{er}$ by binding to and displacing BCL-2 from IP3R-1, where this antiapoptotic protein directly or indirectly controls the phosphorylation status and Ca^{2+} leak through this channel. Overexpressed BCL-2 has been reported to bind and sequester calcineurin, a proposed phosphatase for IP3R (35), which could

represent a possible path by which BCL-2 could indirectly regulate IP3R-1 phosphorylation.

When overexpressed in WEHI7.2 T cells, BCL-2 was recently reported to interact with the IP3 receptors (types 1, 2, and 3) and to inhibit IP3-mediated calcium release from the ER, independent of any measurable effects on intracellular calcium stores (26). These same authors also reported that recombinant BCL-2 reduced the open probability of purified IP3R-1 when reconstituted into lipid bilayers. On the other hand, our genetic dissection of the ER Ca^{2+}-leak pathway controlled by BAX and BAK clearly pointed to a specific role for IP3R-1 and not for IP3R-3. Our results, in combination with the work of Distelhorst and colleagues (26), raise the interesting possibility that selected isoforms of IP3R are used by BCL-2 family members to regulate the amount of Ca^{2+} released from the ER in different ways. The functional consequences of these interactions may depend on BCL-2 expression levels, on the presence of multidomain proapoptotics, or on unidentified cellular factors that cannot be reproduced in lipid bilayer experiments.

Importantly, RNAi reduction of both IP3R-1 and BCL-2 resulted in no additional increase in $[Ca^{2+}]_{er}$ beyond singly knocking down either protein, suggesting that these proteins work in a linear pathway to regulate ER Ca^{2+}. These genetic studies indicate that the ratio of proapoptotic BAX and BAK to antiapoptotic BCL-2 appears to be a critical determinant of the phosphorylation status of IP3R-1 and ER Ca^{2+} stores. In concert, our results support the argument that, in the absence of BAX and BAK, unopposed BCL-2 leads to IP3R-1 hyperphosphorylation, enhanced ER Ca^{2+} leak, and decreased steady-state ER Ca^{2+} stores.

The antibody specific for phosphorylated serine-1755 of IP3R-1 was a kind gift from Dr. S. H. Snyder (The Johns Hopkins University, Baltimore). We thank Y. Nakatani for critical review of our manuscript and E. Smith for manuscript preparation. This research was supported in part by National Institutes of Health Grants K08 AI054650 (to S.A.O.) and R37 CA50239 (to S.J.K.). Work in the laboratory of L.S. is supported by Telethon, Italy, Associazione Italiana per la Ricerca sul Cancro (Italy), and Human Frontier Science Program Organization.

1. Ferri, K. F. & Kroemer, G. (2001) *Nat. Cell Biol.* **3,** E255–E263.
2. Adams, J. M. & Cory, S. (1998) *Science* **281,** 1322–1326.
3. Orrenius, S., Zhivotovsky, B. & Nicotera, P. (2003) *Nat. Rev. Mol. Cell Biol.* **4,** 552–565.
4. Hajnoczky, G., Robb-Gaspers, L. D., Seitz, M. B. & Thomas, A. P. (1995) *Cell* **82,** 415–424.
5. Rizzuto, R., Pinton, P., Carrington, W., Fay, F. S., Fogarty, K. E., Lifshitz, L. M., Tuft, R. A. & Pozzan, T. (1998) *Science* **280,** 1763–1766.
6. Gunter, T. E., Buntinas, L., Sparagna, G., Eliseev, R. & Gunter, K. (2000) *Cell Calcium* **28,** 285–296.
7. Bernardi, P. (1999) *Physiol. Rev.* **79,** 1127–1155.
8. Pinton, P., Ferrari, D., Magalhaes, P., Schulze-Osthoff, K., Di Virgilio, F., Pozzan, T. & Rizzuto, R. (2000) *J. Cell Biol.* **148,** 857–862.
9. Foyouzi-Youssefi, R., Arnaudeau, S., Borner, C., Kelley, W. L., Tschopp, J., Lew, D. P., Demaurex, N. & Krause, K. H. (2000) *Proc. Natl. Acad. Sci. USA* **97,** 5723–5728.
10. Nutt, L. K., Pataer, A., Pahler, J., Fang, B., Roth, J., McConkey, D. J. & Swisher, S. G. (2002) *J. Biol. Chem.* **277,** 9219–9225.
11. Scorrano, L., Oakes, S. A., Opferman, J. T., Cheng, E. H., Sorcinelli, M. D., Pozzan, T. & Korsmeyer, S. J. (2003) *Science* **300,** 135–139.
12. Putney, J. W., Jr., Broad, L. M., Braun, F. J., Lievremont, J. P. & Bird, G. S. (2001) *J. Cell Sci.* **114,** 2223–2229.
13. Vanden Abeele, F., Skryma, R., Shuba, Y., Van Coppenolle, F., Slomianny, C., Roudbaraki, M., Mauroy, B., Wuytack, F. & Prevarskaya, N. (2002) *Cancer Cell* **1,** 169–179.
14. Li, C., Fox, C. J., Master, S. R., Bindokas, V. P., Chodosh, L. A. & Thompson, C. B. (2002) *Proc. Natl. Acad. Sci. USA* **99,** 9830–9835.
15. Schlesinger, P. H., Gross, A., Yin, X. M., Yamamoto, K., Saito, M., Waksman, G. & Korsmeyer, S. J. (1997) *Proc. Natl. Acad. Sci. USA* **94,** 11357–11362.
16. Cameron, A. M., Steiner, J. P., Roskams, A. J., Ali, S. M., Ronnett, G. V. & Snyder, S. H. (1995) *Cell* **83,** 463–472.
17. Nakade, S., Rhee, S. K., Hamanaka, H. & Mikoshiba, K. (1994) *J. Biol. Chem.* **269,** 6735–6742.
18. Grynkiewicz, G., Poenie, M. & Tsien, R. Y. (1985) *J. Biol. Chem.* **260,** 3440–3450.
19. Pieper, A. A., Brat, D. J., O'Hearn, E., Krug, D. K., Kaplin, A. I., Takahashi, K., Greenberg, J. H., Ginty, D., Molliver, M. E. & Snyder, S. H. (2001) *Neuroscience* **102,** 433–444.
20. Camello, C., Lomax, R., Petersen, O. H. & Tepikin, A. V. (2002) *Cell Calcium* **32,** 355–361.
21. Taylor, C. W. & Laude, A. J. (2002) *Cell Calcium* **32,** 321–334.
22. Patel, S., Joseph, S. K. & Thomas, A. P. (1999) *Cell Calcium* **25,** 247–264.
23. Wagner, L. E., II, Li, W. H., Joseph, S. K. & Yule, D. I. (2004) *J. Biol. Chem.* **279,** 46242–46252.
24. Cheng, E. H., Wei, M. C., Weiler, S., Flavell, R. A., Mak, T. W., Lindsten, T. & Korsmeyer, S. J. (2001) *Mol. Cell* **8,** 705–711.
25. Distelhorst, C. W. & Shore, G. C. (2004) *Oncogene* **23,** 2875–2880.
26. Chen, R., Valencia, I., Zhong, F., McColl, K. S., Roderick, H. L., Bootman, M. D., Berridge, M. J., Conway, S. J., Holmes, A. B., Mignery, *et al.* (2004) *J. Cell Biol.* **166,** 193–203.
27. Lomax, R. B., Camello, C., Van Coppenolle, F., Petersen, O. H. & Tepikin, A. V. (2002) *J. Biol. Chem.* **277,** 26479–26485.
28. Van Coppenolle, F., Vanden Abeele, F., Slomianny, C., Flourakis, M., Hesketh, J., Dewailly, E. & Prevarskaya, N. (2004) *J. Cell Sci.* **117,** 4135–4142.
29. Sugawara, H., Kurosaki, M., Takata, M. & Kurosaki, T. (1997) *EMBO J.* **16,** 3078–3088.
30. Hofer, A. M., Curci, S., Machen, T. E. & Schulz, I. (1996) *FASEB J.* **10,** 302–308.
31. Hamman, B. D., Hendershot, L. M. & Johnson, A. E. (1998) *Cell* **92,** 747–758.
32. Bassik, M. C., Scorrano, L., Oakes, S. A., Pozzan, T. & Korsmeyer, S. J. (2004) *EMBO J.* **23,** 1207–1216.
33. Cheng, E. H., Sheiko, T. V., Fisher, J. K., Craigen, W. J. & Korsmeyer, S. J. (2003) *Science* **301,** 513–517.
34. Danial, N. N., Gramm, C. F., Scorrano, L., Zhang, C. Y., Krauss, S., Ranger, A. M., Datta, S. R., Greenberg, M. E., Licklider, L. J., Lowell, B. B., *et al.* (2003) *Nature* **424,** 952–956.
35. Shibasaki, F., Kondo, E., Akagi, T. & McKeon, F. (1997) *Nature* **386,** 728–731.